

Comparative study in use sodium silicate instead of NH_4OH as an alkaline basic catalyst to gelation unmodified silica aerogel based on tetraethoxysilane (TEOS)

Z. H. A. Al-Mothafer*, I. M. Abdulmajeed*

Physics Department, College of Science, University of Baghdad, Iraq

In the present work, nonporous hydrophilic unmodified silica aerogel was synthesized successfully by ambient drying with one step base catalyst by used silica organic initiator tetraethoxysilane (TEOS). Silica aerogel was prepared twice by sol-gel technique; the first one was the gelation that happened under the alkaline catalyst NH_4OH , which has a toxic property and dangerous to human health. The second gelation under the effect of the safety inorganic base catalyst sodium silicate (water glass) that used as an inorganic low-cost and environmentally friendly initiator to silica, plays a role in increasing pH as a catalyst and as a new rare co-precursor mixing organic and inorganic silica precursors ($\text{TEOS} + \text{Na}_2\text{SiO}_3$). The impurities accompanying water glass and sodium residue were eliminated by a lot of washing. The volume ratio of the (TEOS: ethanol: H_2O : base catalyst) fixed respectively at (5.6:50:10:0.01M). The gelation reaction time, the gel properties, its quality and the amount of the reactant, the density, and the appearance all effect by the type of catalyst used. The comparative study of silica porous aerogel production properties diagnostic achieved by FTIR, XRF, BET, BJH, FESEM and thermal conductivity applied as insulation materials.

(Received April 8, 2021; Accepted August 2, 2021)

Keywords: Silica aerogel, Sodium silicate as a solid base alkaline catalyst, Co-precursors, Thermal insulation materials

1. Introduction

Silica aerogel possesses a porous nanostructure's properties giving it low density, high surface area with very reliable thermal insulation [1–4]. Many practical applications depend on its properties, like thermal insulators, hypervelocity particles, extracts, and adsorbents agent [5–7]. The silica production was done using the sol-gel process method that included the reaction of the water with the silica precursor with present the solvent like acetone or ethanol with essential catalyst supercritical drying in the final stage [2]. The supercritical drying method is included removing the solvent at the critical pressure and temperature. The supercritical drying method has several aspects of safety and cost, leading to limiting silica aerogel production. Drying of the wet gels at the standard pressure [2]. The silica aerogels are made from two types of silicon precursor. The silicon precursors have included organosilane that including (tetraethoxysilane TMOS, methyl-hydro siloxane PMHS [8–11] or Na_2SiO_3 [12–15].

Some studies showed that a tetraethoxysilane TEOS does Preparation of the wet gels, but it showed cracks and could break for small pieces under the normal pressure, and the wet gels produced from xerogels [16–17]. [13–15] prepared the water glass-based aerogels in vapour passing technique or ion exchange techniques that included removing the sodium from the water glass. This technique needs several hours for sodium removal.

Many studies found a co-precursor technique is used to produce hydrophobic silica aerogels by (Hexadecyltrimethoxysilane with tetraethoxysilane or dimethyl diethoxy silane with tetraethoxysilane [18–21]. Characterization and synthesis of silica aerogels are done by (organic+inorganic) such as silica sol and tetraethoxysilane [22].

Our article included production silica aerogels without Surface changing using ($\text{TEOS} + \text{Na}_2\text{SiO}_3$) and drying it at the normal pressure. The silica sols are colloidal liquid consisting of single nanoparticles such as (SiO_2) with a hydroxylated surface. It is making them dissolved in

* Corresponding authors: inaam.mohammed@sc.uobaghdad.edu.iq

water without sedimentation. The gel solution is stay stabilized by cations (such as sodium) (alkaline). Alkaline silica sol increasing pH without needing ion exchange as comparing to the water glass. The report gives a basis for the distribution of hydrophilic silica aerogel made by co-precursor [22].

Comparing it with silica gel prepared by ammonium hydroxide is commonly used as a base catalyst with very Risks and warnings associated with the use of ammonia hydroxide jet smell causes severe damage to the respiratory system of human as illustrate at hazardous substance fact sheet [23].

2. Experimental procedures

2.1. Materials

TEOS (Sigma-Aldrich 98%) is used as a precursor. ($\text{Na}_2\text{SiO}_3 \cdot 5\text{H}_2\text{O}$) sodium metasilicate pentahydrate (LR THOMAS BAKR India) used as precursors and catalyst. NH_3 Sigma-Aldrich 37% used as a base catalyst. Double-distilled water was used to solve sodium silicate and NH_3 . Ethanol AR 100% ($\text{C}_2\text{H}_5\text{OH}$ Alpha chemical India and N-Hexan, 96%, analytical grade, ASC Scharlau chemical Company both used as solvent exchange. N, N-Dimethylformamide, DMF, NSC 5356 Sigma-Aldrich, used as a chemical control drying agent CCDA.

2.2 preparation of silica aerogels:

0.5 M of the organic initiator TEOS was dissolved in 50 mL ethanol in two plastic containers (A) and (B) for 24 hours and then placed on a rapid stirrer for 1 hour at 50°C with the chemical control drying agent CCDA N, N-Dimethylformamide, DMF to the sol.

Ammonia hydroxide was dropped in a container (A), and the sodium silicate was dropped in a container (B). Container (A) gelation occur after 18 min with water product and semi-coherent and transparent gel. Container (B) gelation occur faster after 12 min without water product complete interaction with the forming coherent spongy nature gel—both containers aged 24 hours at 50° to complete reaction strengthening the internal structure.

Container (A) directly was entered the solvent exchanging stage from hydrogel (water filled the porous) to Alcolgel (alcohol-filled porous) by replacing water with ethanol for 48 hours. Then replace ethanol with hexane for 48 hours, too, until it reaches the drying stage for seven days in a closed container at the ambient temperature. Finally, the calcination stage includes a slow, gradual rise in temperature up to 120°C for two hours, as shown in diagram 1.

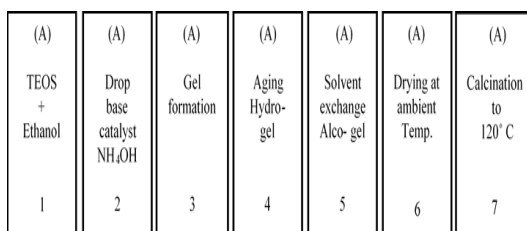


Fig. 1. Diagram of silica aerogel preparation steps using ammonium hydroxide as a base catalyst in container (A).

Container (B), a purification step is required to remove the impurities associated with the metasilicate containing sodium ion, preceding the stage of replacing the solutions from the hydrogel to the alcolgel, as shown in diagram 2.

(B)	(B)	(B)	(B)	(B)	(B)	(B)	(B)
TEOS + Ethanol	Drop base catalyst 1 Na ₂ SiO ₃	Gel formation	Aging Hydro-gel	Washing and purification	Solvent exchange Alco-gel	Drying at ambient Temp.	Calcination at 120°C
1	2	3	4	5	6	7	8

Fig. 2. Diagram of silica aerogel preparation steps using Sodium metasilicate as a base catalyst in the container (B).

2.3. Characterizations

The aerogels' characterization includes volume shrinkage, pore-volume, density, Scanning Electron Spectroscopy, Infrared ray, thermal conductivity, pore size, and distribution measurements. Determination of the volume shrinkage, pore by follows [24]:

$$\text{Volume shrinkage}\% = \frac{1-V_a}{V_g} \quad (1)$$

$$\text{Porosity \%} = 1 - \left(\frac{\rho_b}{\rho_s}\right) \times 100\% \quad (2)$$

$$\text{Pore volume} = \left(\frac{1}{\rho_b} - \frac{1}{\rho_s}\right) \text{ cm}^3 / \text{g} \quad (3)$$

V_a, V_g is volume of hydrogel and aerogel respectively, (s) is solid silica, (b) represents silica aerogel; ρ_b, ρ_s are solid silica densities.

The thermal conductivity was calculated by C–T meter (Teleph, France) through the ring probe in the aerogel). To calculate thermal conductivity (k) using the following equation [24]:

$$T = \frac{I^2 R}{L.4\pi K(\ln(t)+C)} \quad (4)$$

R represents resistance of the heater

t represent the pulse time

c is the integration constant

I mean, the current of the probe wire

K represents the thermal conductivity of the sample

L represents the length of the heater

The aerogel's chemical components were confirmed with Fourier Transform Infrared Spectroscopy (FTIR) using IRAffinity-1 SHIMAZU in the Sharif University of Technology Tehran, 400–4,000 cm⁻¹ range Spectrophotometer.

The silica aerogels' microstructure was found with (FESEM) Toscana Zeiss-EM10C-100 KV.

The ratio of the mass does calculation of the silica aerogels densities to the volume. The density involved interparticle voids and pores with porosity, calculated by (2), [22, 23].

$$\rho_s = 2.19 \text{ g}\cdot\text{cm}^{-3}$$

Analysis of BET surface area was done by determining the sample's surface areas by absorption of nitrogen at (77) K. the samples were kept under vacuum for two hours and heated at (120) °C for removing all the volatile substances. The BJH technique determines pore size and pore volume. The pore structures showed nitrogen adsorption.

The percentage of components and content of elements analysis for each sample diagnosed by the device X-ray fluorescent XRF. SPECTRO XEPOS. Philips, model PW 2404 and 1480.

3. Results

3.1. The gelation Time and Bulk Density

Table 1. The physical properties of the prepared samples with different catalyst.

sample name	The catalyst	Density g/cm ³	Porosity %	Shrinkage %	Gelation time (min.)	The appearance	Final shape
TBI	NH ₄ OH	0.17	89%	68%	18	Transparency without cracks	
CBI	Na ₂ SiO ₃	0.09	87%	73%	8	Less Transparency without cracks	

3.2. FTIR Analysis

The recorded IR transmitted spectrum for the unmodified prepared aerogel samples with different catalyst are shown in Fig.(3), the details summarized in Table (2). Several absorption bands are marking out in these spectra due to their interest in our study. There were no apparent differences between the two samples except the appearance 1401.36 related to organic compound conjugated to use both chemical control drying agent CCDA DMF C₃H₇NO and related to organic silicon initiators TEOS SiC₄H₁₂O₄. There are different intensity decreases with CBI sample because of the complete condensation reaction and more dense polymerization chains. The philic properties confirm in hydrogen-bonded water (3427 cm⁻¹) and physically absorbed water production silicon bands (1632 cm⁻¹),(958 cm⁻¹) are present. Still, without Si-C and -CH₃, indicating that the unmodified silica aerogel mesosphere is hydrophilic Intensity of the O-H is hydrophilic due to the Surface covering the hydroxide [26-29].

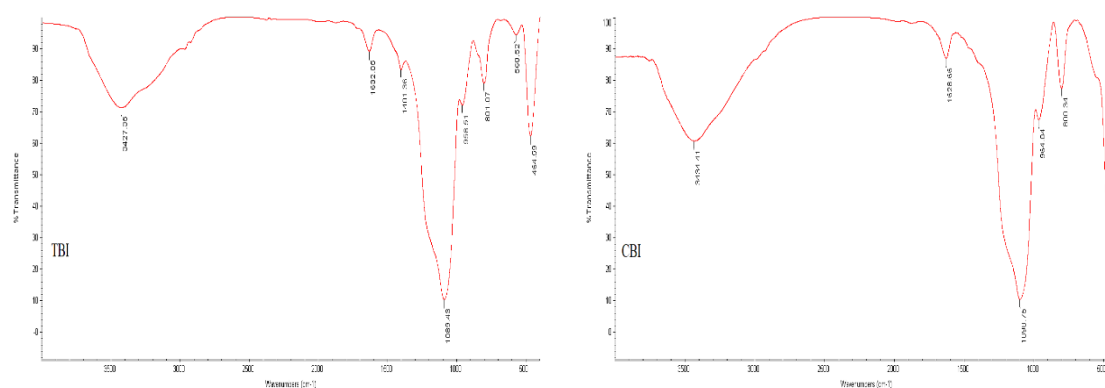


Fig. 3. FTIR spectrum of (TBI) aerogel with NH₄OH catalyst, (CBI) aerogel with Na₂SiO₃ catalyst.

Table 2. Detail bands diagnosed with an FTIR technique to aerogel samples.

Wave numbers(cm^{-1})		Group type [25,26]
TBI	CBI	
446.59	466.53	Strong Si-O-Si
801.07	800.34	Si-O-Si stretching vibration
958.51	964.04	Weak Si-OH
1089.43	1089.75	Potential and Si-O-Si stretching depended on the structure of the silica
1401.36	compound N=N stretching, First overtone N-H stretching, first overtone O-H stretching, Combination C-H stretching Common near-infrared bands silicon-organic compounds stretching silicon compound
1632.05	1628.66	The weak peak Si-OH
3427.36	3434.41	The broad peak O-H

3.3. XRF analysis

A result of the component percentage analysis of silica aerogel-based organic initiators prepared under different catalyst influences. The excellent results regarding the amount of pure silica free from any mineral compounds are associated with the meta-sodium silicate due to the washing step that worked and followed the gelation step that led to a very pure product shown in Table (3).

Table 3. Results XRF component percentage of the aerogel samples.

The Sample	The catalyst	The component percentage %
TBI	NH_4OH	100% SiO_2
CBI	Na_2SiO_3	100% SiO_2

3.4. FESEM analysis

The FESEM pictures shown in Fig. (4) was found that the size of the pore and particle of both samples are tiny (semi equal converging in the dimensions 20-50 nm for both samples because they prepared with the same concertation in (precursors: Ethanol: water: catalyst)). The examples' optical transparency appearance is shown in Table (1) of the aerogel that showed a slight decrease in sample CBI because Na_2SiO_3 catalyst has metal impurities (Sodium Meta-silicate). Besides, it has intensive condensation reaction, and the absence of surface modification led to more formation Si-OH groups in the pores and Surface.

The microstructures consist of spherical particles aggregate in clusters produce pore sizes in narrow diameters in the range less of slight contact in the neck region between the particles. Particle size very homogeneous in shapes and diameter. Perfect connectivity among the particles results in aerogel with monolithic nature with high mechanical strength. The size of the particles practically is not affected by the catalyst type; homogeneous particles are observed. Hard agglomerates can affirm that uniform-sized silica particle. Also, clusters of the particles are reacted with Brownian motion, and siloxane bridges increase and reinforcing the silica network in neck regions [30].

The white and black Surface of the aerogel is bulges and pores, respectively. The images showed that the prepared aerogels are porous materials with pore sizes in the nanoscale range; in other meaning, particles size is less than one hundred nanometers.

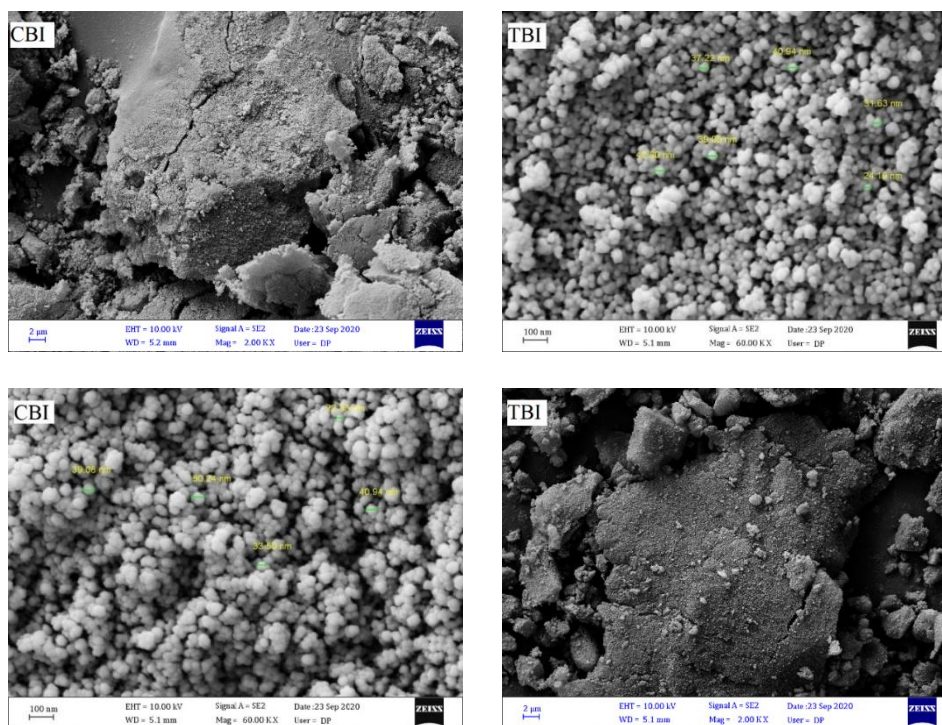


Fig. 4. SEM for TBI mesopores aerogel with NH_4OH catalyst, (CBI) mesopores aerogel with Na_2SiO_3 catalyst, at different magnification

3.5. BET analysis

Surface area, pore size, and pore volume are determined using BET. BJH techniques represented gas adsorption, a well-established tool for characterizing the texture of porous solids and fine powders, a wide range of pores (2-50) nm named mesopores. The pores' condensation is included and converted to liquid form at a pressure p more minor than the saturation pressure p_s such as pores condensation showed a vapour-liquid transforming in specific volume. Pore condensation is not used for micropore filling because it does not include vapour-liquid transition [31].

Fig. (5) Shows the linear isotherm plots for aerogel samples with NH_4OH and Na_2SiO_3 base catalyst, respectively. Those with diameters between 14 and 32 nm are termed "mesopores". The shape and size of the hysteresis loop could be used qualitatively for types of pores encountered by nitrogen during a sorption trial.

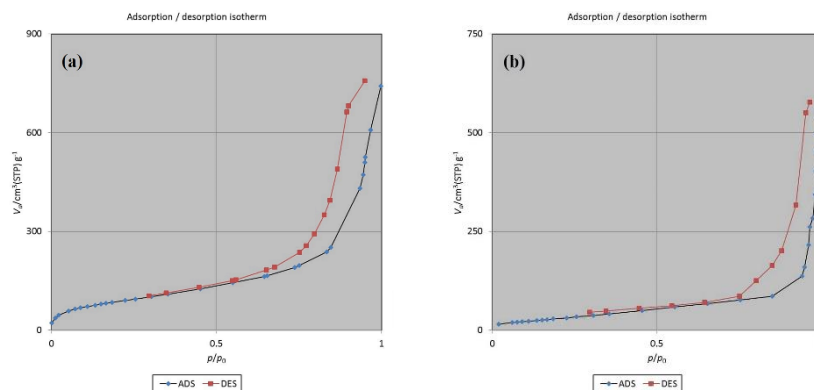


Fig. 5. The hysteresis loops for silica aerogel with different catalyst (a) NH_4OH , (b) Na_2SiO_3 .

Monolayer adsorption occurs at lower pressures; the inflection point occurs after the first monolayer as fig.5 occurs fast at 0.75 with NH_4OH catalyst while at 0.85 with Na_2SiO_3 catalyst. At higher pressures, the slope shows increased uptake of adsorbate as pores become filled. In all samples, the multilayer transitions occur with a pseudo-plateau region indicative of near-complete filling of the mesopores.

The plots fall into two behaviours according to their adsorption manners. The plots in the first have a linear relative behaviour. Then take a deflection as the values of relative pressure increase with notice an increase in the volume of adsorbed gas. The silica aerogel demonstrates a similar type of adsorption-desorption isotherm (H3) related to non-rigid aggregates of plate-like particles as Fig.6 [31].

The reaction rate is too effective to form a high crosslinked network structure, leading to the aerogel's low specific surface area [31]. Therefore, sample cbi Na_2SiO_3 catalyst has a low specific surface area ($110 \text{ m}^2 \cdot \text{g}^{-1}$) as illustrating in Table (3) and (4), Where it shows less quantity of gas adsorbed ($550 \text{ cm}^3/\text{g STP}$) than sample tbi NH_4OH catalyst has ($317 \text{ m}^2 \cdot \text{g}^{-1}$, $800 \text{ cm}^3/\text{g STP}$). In general, as expected by Iler [33], the surface area of silica aerogels is decreased as the final preparation pH value increased, that what happened with Na_2SiO_3 catalyst sample cbi reached 9 pH.

The higher porosity occurred in the tbi sample 89%, while the lowest porosity was 87%, founded in the cbi sample. This may be attributed to the less shrinking from gel to aerogel with sample tbi NH_4OH catalyst, and leads to decreasing density and increasing the volume and high porosity with high total pore volume and small mean pore diameter, Then the quantity of gas adsorbed against the greater surface area, consequently their large total pore volume.

Pore diameter, Surface area and total pore volume determine through nitrogen adsorption-desorption test using BET, BJH technique shown in table (4) for the prepared samples with different base catalyst. The total pore volume increases, the bulk density decreases because the increase in porosity means more monolith volume with a large amount of air, in the other hands, an increase in volume with weight loss, which means a decrease in the density. When the gel network is exposed to pressure, shrinkage is due to producing the aerogel in the specific area. The total pore volume directly proportional to the particular surface area.

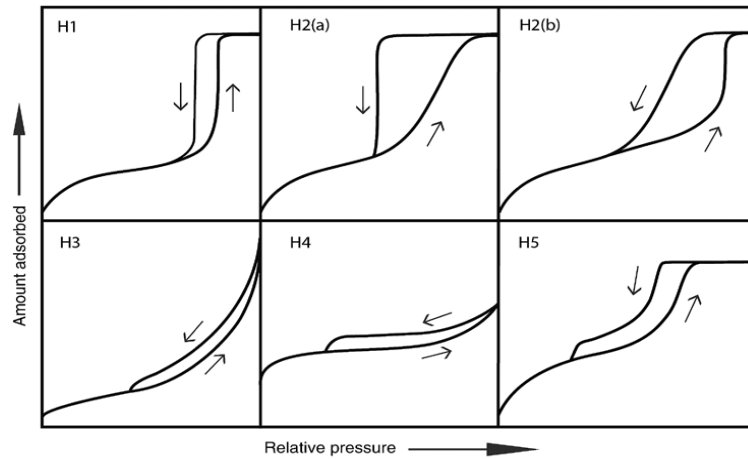


Fig. 6. Classification of hysteresis loops [31].

Table 4. Surface area, pore diameter, and total pore volume determined by nitrogen adsorption test by using BET, BJH method.

Sample	Catalyst	BET			BJH		Porosity %
		Mean pore Diameter (nm)	surface Area (cm ² /g)	Total pore Vol. (cm ³ /g)	Total pore Vol. (cm ³ /g)	specific Surface area (m ² /g)	
TBI	NH ₄ OH	14.118	317.38	1.1202	1.1106	326.95	89%
CBI	Na ₂ SiO ₃	32.012	110.59	0.885	0.8876	130.13	87%

3.6. Thermal Conductivity

Figure (7) shows low range of thermal conductivity (0.228–0.396W. m⁻¹k⁻¹) by adding NH₄OH as a catalyst (TBI samples) at ambient pressure aerogel, while the value of the thermal conductivity is important and in range (0.15-0.5 W.m⁻¹ k⁻¹) for using sodium silicate as a catalyst addition (CBI samples), this is due to the 89% porosity of (TBI) samples compared with 87% CBI samples. All these acceptable results aerogels used as highly insulating materials.

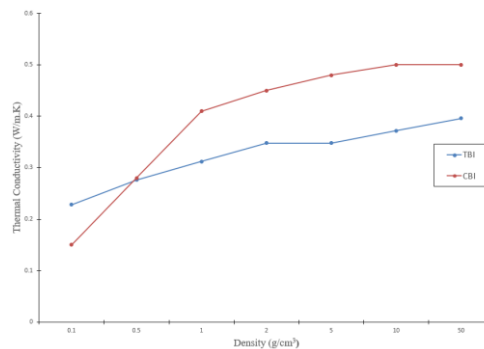


Fig. 7. Thermal conductivity for aerogel with different catalysts; (TBI) aerogel with NH₄OH catalyst, (CBI) aerogel with Na₂SiO₃ catalyst.

4. Conclusion

Hydrophilic silica aerogels were obtained successfully and drying at ambient pressure using two techniques. The first one: NH_4OH is a catalyst to gelation Tetraethoxysilane (TEOS) and second: sodium silicate (Na_2SiO_3) as a catalyst to gelation Tetraethoxysilane (TEOS), respectively to produce unmodified silica aerogel with one step base catalyst method. The gelation reaction time, the gel properties, quality and the amount of the reactant, the density, and the appearance all parameters effect by the type of catalyst used.

Aerogel samples with a high porosity already exhibit low thermal conductivity for NH_4OH used as catalyst compared with pores samples of Na_2SiO_3 , so the aerogels could use for insulating. The most critical application of aerogels is in all types of thermal insulation.

Silica aerogels with Na_2SiO_3 as a catalyst have physical and environmental advantages, non-toxic, easy to handle, and nonflammable compared with the NH_4OH catalyst.

References

- [1] M. Schmidt, F. Schwertfeger, *J. Non-Cryst. Solids* **225**, 364 (1998).
- [2] M. A. Aegerter, N. Leventis, M. M. Koebel, *Aerogels, Handbook*, Springer, New York, (2011).
- [3] J. Fricke, A. Emmerling, *Aerogels, J. Am. Ceram. Soc.* **75**, 2027 (1992).
- [4] M. Reim, G. Reichenauer, W. Korner, J. Manara, M. Arduini-Schuster, S. Korder, A. Beck, J. Fricke, *J. Non-Cryst. Solids* **350**, 358 (2004).
- [5] M. Tabata, I. Adachi, Y. Hatakeyama, H. Kawai, T. Morita, T. Sumiyoshi, *J. Supercrit. Fluids* **110**, 183 (2016).
- [6] M. Alnaief, S. Antonyuk, C.M. Hentzschel, C.S. Leopold, S. Heinrich, I. Smirnova, *Microporous Mesoporous Mater.* **160**, 167 (2012).
- [7] S. M. Jones, *J. Sol-Gel Sci. Technol.* **40**, 351 (2006).
- [8] A. V. Rao, R. R. Kalesh, *Sci. Technol. Adv. Mater.* **4**, 509 (2003).
- [9] A. V. Rao, M. M. Kulkarni, *Mater. Res. Bull.* **37**, 1667 (2002).
- [10] S. D. Bhagat, A. V. Rao, *Appl. Surf. Sci.* **252**, 4289 (2006).
- [11] B. N. Nguyen, M. A. Meador, A. Medoro, V. Arendt, J. Randall, L. McCorkle, B. Shonkwiler, *ACS Appl. Mater. Interfaces* **2**, 1430 (2010).
- [12] Z. H. A. Al-Mohtafar, I. M. Abdulmajeed, I. F. AL-Sharuee, *J. of Ovonic Research* **17**, 175 (2021).
- [13] M. A. Einarsrud, E. Nilsen, *J. Non-Cryst. Solids* **226**, 122 (1998).
- [14] A. P. Rao, A. V. Rao, G. M. Pajonk, P. M. Shewale, *J. Mater. Sci.* **42**, 8418 (2007).
- [15] P. M. Shewale, A. V. Rao, J. L. Gurav, A. P. Rao, *J. Porous. Mater.* **16**, 101 (2009).
- [16] L. Durães, M. Ochoa, N. Rocha, R. Patrício, N. Duarte, V. Redondo, A. Portugal, *J. Nanosci. Nanotechnol.* **12**, 6828 (2012).
- [17] D. L. Meixner, P. N. Dyer, *J. Sol-Gel Sci. Technol.* **14**, 223 (1999).
- [18] A. V. Rao, M. M. Kuakarni, *J. Sol-Gel Sci. Technol.* **27**, 103 (2003).
- [19] B. Zhou, J. Shen, Y. H. Wu, G. M. Wu, X. Y. Ni, *Mater. Sci. Eng. C* **27**, 1291 (2007).
- [20] L. A. Capadona, M. A. B. Meador, A. Alunni, E. F. Fabrizio, P. Vassilaras, N. Leventis, *Polymer* **47**, 5754 (2006).
- [21] N. D. Hegde, A. V. Rao, *Appl. Surf. Sci.* **253**, 1566 (2006).
- [22] Ming Li, Hongyi Jiang, Dong Xu, Ou Hai, Wei Zheng, *Journal of Non-Crystalline Solids* **452**, 187 (2016).
- [23] J. Vincent Nabholz, *Science of The Total Environment* **109–110**, 649 (1991).
- [24] A. Parvathy Rao, A. Venkateswara Rao, Jyoti L. Gurav, *J Porous Mater* **15**, 507 (2008).
- [25] Valeri P. Tolstoy, Irina V. Chernyshova, Valeri A. Skryshevsky, *Handbook of Infrared Spectroscopy of Ultrathin Films*, Copyright, John Wiley & Sons, Inc., Hoboken, New Jersey, ISBN: 978-0-471-35404-8 (2003).
- [26] Barbara H. Stuart, University of Technology, Sydney, Australia, *Infrared Spectroscopy: Fundamentals And Applications*, John Wiley, Ltd.(2004).

- [27] Ashraf M. Alattar, Matthew Drexler, Wesam A. A. Twej, Faisal M. Alamgir, Structural and luminescent properties of a NaYF₄-aerogel composite, 1569-4410, Elsevier, (2018).
- [28] Zh. V. Faustova, Yu. G. Slizhov, Inorganic Materials **53**(3), 287 (2017).
- [29] Qifeng Chen, Hui Wang, Luyi Sun, Materials **10**, 435 (2017).
- [30] Azadeh Tadjarodi, Marzieh Haghverdi, Vahid Mohammadi, Materials Research Bulletin, (2012).
- [31] Matthias Thommes, Katsumi Kaneko, Alexander V. Neimark, Pure Appl. Chem. **87**(9-10), 1051 (2015).
- [32] Bahaa F. Shihab, Wesam A A Twej, International Journal of Advanced Research in Science, Engineering and Technology **5**(7), (2018).
- [33] G. B. Khomutov, Yu. A. Koksharov, Advances in Colloid and Interface Science **122**(1-3), 119 (2006).